A Letters Journal Exploring
the Frontiers of Physics

OFFPRINT

Optical flux lattices for two-photon dressed states

N. R. Cooper and J. Dalibard

EPL, **95** (2011) 66004

epl

A Letters Journal Exploring the Frontiers of Physics

AN INVITATION TO SUBMIT YOUR WORK

www.epljournal.org

The Editorial Board invites you to submit your letters to EPL

EPL is a leading international journal publishing original, high-quality Letters in all areas of physics, ranging from condensed matter topics and interdisciplinary research to astrophysics, geophysics, plasma and fusion sciences, including those with application potential.

The high profile of the journal combined with the excellent scientific quality of the articles continue to ensure EPL is an essential resource for its worldwide audience. EPL offers authors global visibility and a great opportunity to share their work with others across the whole of the physics community.

Run by active scientists, for scientists

EPL is reviewed by scientists for scientists, to serve and support the international scientific community. The Editorial Board is a team of active research scientists with an expert understanding of the needs of both authors and researchers.

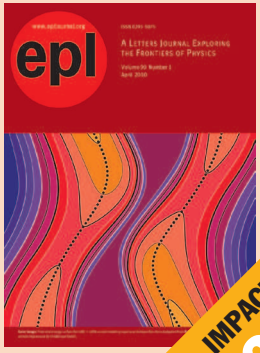

IMPACT FACTOR 2.753*

*As ranked by ISI 2010

IMPACT FACTOR
2.753*
* As listed in the ISI® 2010 Science Citation Index Journal Citation Reports

OVER
500 000
full text downloads in 2010

30 DAYS
average receipt to online publication in 2010

16 961
citations in 2010
37% increase from 2007

"We've had a very positive experience with EPL, and not only on this occasion. The fact that one can identify an appropriate editor, and the editor is an active scientist in the field, makes a huge difference."

Dr. Ivar Martinv
Los Alamos National Laboratory, USA

Six good reasons to publish with EPL

We want to work with you to help gain recognition for your high-quality work through worldwide visibility and high citations.

1. **Quality** – The 40+ Co-Editors, who are experts in their fields, oversee the entire peer-review process, from selection of the referees to making all final acceptance decisions
2. **Impact Factor** – The 2010 Impact Factor is 2.753; your work will be in the right place to be cited by your peers
3. **Speed of processing** – We aim to provide you with a quick and efficient service; the median time from acceptance to online publication is 30 days
4. **High visibility** – All articles are free to read for 30 days from online publication date
5. **International reach** – Over 2,000 institutions have access to EPL, enabling your work to be read by your peers in 100 countries
6. **Open Access** – Articles are offered open access for a one-off author payment

Details on preparing, submitting and tracking the progress of your manuscript from submission to acceptance are available on the EPL submission website **www.epletters.net**.

If you would like further information about our author service or EPL in general, please visit **www.epljournal.org** or e-mail us at **info@epljournal.org**.

EPL is published in partnership with:

European Physical Society | Società Italiana di Fisica | EDP Sciences | IOP Publishing

A Letters Journal Exploring the Frontiers of Physics

September 2011

EPL, **95** (2011) 66004
doi: 10.1209/0295-5075/95/66004

www.epljournal.org

Optical flux lattices for two-photon dressed states

N. R. Cooper[1] and J. Dalibard[2]

[1] *T.C.M. Group, Cavendish Laboratory - J. J. Thomson Avenue, Cambridge CB3 0HE, UK*
[2] *Laboratoire Kastler Brossel, CNRS, UPMC, Ecole Normale Supérieure - 24 rue Lhomond, 75005 Paris, France*

received 4 June 2011; accepted in final form 1 August 2011
published online 7 September 2011

PACS 67.85.-d – Ultracold gases, trapped gases
PACS 03.65.Vf – Phases: geometric; dynamic or topological
PACS 73.43.-f – Quantum Hall effects

Abstract – We describe a simple scheme by which "optical flux lattices" can be implemented in ultracold atomic gases using two-photon dressed states. This scheme can be applied, for example, to the ground-state hyperfine levels of commonly used atomic species. The resulting flux lattices simulate a magnetic field with high mean flux density, and have low-energy bands analogous to the lowest Landau level. We show that in practical cases the atomic motion significantly deviates from the adiabatic following of one dressed state, and that this can lead to significant interactions even for fermions occupying a single band. Our scheme allows experiments on cold atomic gases to explore strong correlation phenomena related to the fractional quantum Hall effect, both for fermions and bosons.

There has long been an endeavour in the field of ultracold atomic gases to achieve an experimental regime in which strong correlation phenomena associated with the fractional quantum Hall (FQH) effect can appear [1–3]. Central to this goal is the formation of Landau levels: the highly degenerate energy levels of a two-dimensional charged particle in a uniform magnetic field. Owing to this degeneracy, particles occupying a single Landau level are susceptible to interparticle interactions. These can give rise to strongly correlated FQH states when the particle density is comparable to the density of magnetic flux quanta n_ϕ. Existing experimental studies of FQH states in semiconductors involve fermions (electrons). However it is expected that related strong-correlation phenomena can arise also for bosonic species of cold atoms [3].

The formation of Landau levels for neutral atoms requires the creation of an effective magnetic field. To date, this has been achieved in experiments on ultracold atoms either by using rotation [2,3], or by using optical dressing to generate effective gauge fields [4]. However, in both cases the magnetic flux densities n_ϕ achieved so far are too low to bring a large atom cloud into the fractional quantum Hall regime. Theoretical proposals for methods to generate effective magnetic fields for atoms on deep optical lattices hold promise to achieve high flux densities, on the order of the inverse optical wavelength squared $n_\phi \sim 1/\lambda^2$ (for reviews of these proposals see, *e.g.* [5,6]). At these flux densities, interaction energy scales would be sufficiently large to allow experimental studies even in the FQH regime.

A recent theoretical proposal has shown that effective magnetic fields with high flux density $n_\phi \sim 1/\lambda^2$ can also be generated for optically dressed states without the use of deep optical lattices. In this so-called "optical flux lattice" scheme [7] a periodic effective magnetic field with non-zero average is generated by arranging that the spatial dependence of the Rabi coupling and a state-dependent potential are in register with each other. The implementation proposed in ref. [7] involves a single-photon coupling, suitable for ytterbium or alkaline earth atoms, and requires locking the positions of standing waves of a laser at the coupling frequency with those of a laser at an "antimagic" frequency.

In this paper, we show how optical flux lattices can be generated by using two-photon dressed states. Our scheme also requires two laser frequencies, but it is more robust than that of [7]: the Rabi coupling and state-dependent potential are automatically in register. Importantly, our scheme can be applied to commonly used atomic species, including alkali atoms in hyperfine levels of any angular momentum F. We describe the bandstructures for representative cases $F = 1/2$ and $F = 1$. We show that there appear low-energy bands that are analogous to the lowest Landau level: of narrow width in energy and with non-zero Chern number [8]. Owing to the narrow energy width, particles occupying these bands are susceptible to

interactions and to the formation of strongly correlated FQH states. We show that, even for fermions interacting with contact interactions, there remain significant interparticle interactions within this low-energy band. Thus, our scheme will allow experiments on cold atomic gases to explore strong correlation phenomena related to the fractional quantum Hall effect for both fermions and bosons.

In the first part of this paper we consider an atomic species with a ground level g of angular momentum $J_g = 1/2$. Examples of atoms in this category that have already been laser-cooled are ^{171}Yb or ^{199}Hg (level $6\,^1S_0$) [9,10]. The atoms are irradiated by laser waves of frequency ω_L that connect g to an excited state e also with angular momentum $J_e = 1/2$. For ytterbium and mercury atoms, we can choose e to be the first excited level $6\,^3P_0$ entering in the so-called "optical clock" transition. The very long lifetime of e ($\sim$10 s for Yb [11] and $\sim$1 s for Hg [12]) guarantees that heating due to random spontaneous emissions of photons is negligible on the time scale of an experiment. Another possible choice could be ^{6}Li atoms, but we estimated in this case a photon scattering rate that is too large to maintain the gas at the required low temperature.

We assume that the atomic motion is restricted to the xy-plane and described by the Hamiltonian

$$\hat{H} = \frac{\boldsymbol{p}^2}{2M}\hat{1} + \hat{V}(\boldsymbol{r}), \tag{1}$$

where M is the atomic mass and $\boldsymbol{p}$ its momentum. The matrix $\hat{V}$ acts in the Hilbert space describing the internal atomic dynamics. For an off-resonant excitation, we can assume that the population of e is negligible at all times, so that $\hat{V}$ is a 2×2 matrix acting on the $g_\pm$ manifold [13]. Its coefficients depend on the local value of the laser electric field, which we characterize by the Rabi frequencies κ_m, $m = 0, \pm 1$, where $m\hbar$ is the angular momentum along z gained by the atom when it absorbs a photon.

In order to increase our control on the spatial variations of $\hat{V}$, we suppose that a magnetic field parallel to the z-axis lifts the degeneracy between the states $g_\pm$. The resulting splitting δ is supposed to be much larger than the κ_m's. Hence for a monochromatic laser excitation at frequency ω_L, the off-diagonal matrix elements V_{+-} and V_{-+} are negligible compared to the diagonal ones. However we also assume that another laser field at frequency $\omega_L + \delta$, propagating along the z-axis with σ_- polarization (*i.e.* $m = -1$ with the notation above), is shone on the atoms. The association of this field with the π component ($m = 0$) of the light at ω_L provides the desired resonant Raman coupling between $|g_\pm\rangle$ (fig. 1(a)). Using standard angular momentum algebra we find in the $\{|g_+\rangle, |g_-\rangle\}$ basis:

$$\hat{V} = \frac{\hbar\kappa_{\rm tot}^2}{3\Delta}\hat{1} + \frac{\hbar}{3\Delta}\begin{pmatrix} |\kappa_-|^2 - |\kappa_+|^2 & E\kappa_0 \\ E\kappa_0^* & |\kappa_+|^2 - |\kappa_-|^2 \end{pmatrix}. \tag{2}$$

Here $\kappa_{\rm tot}^2 = \sum_m |\kappa_m|^2$, $\Delta = \omega_L - \omega_A$, where ω_A is the atomic resonance frequency, and we assume $|\Delta| \gg |\delta|, |\kappa_m|$. The quantity E characterizes the field

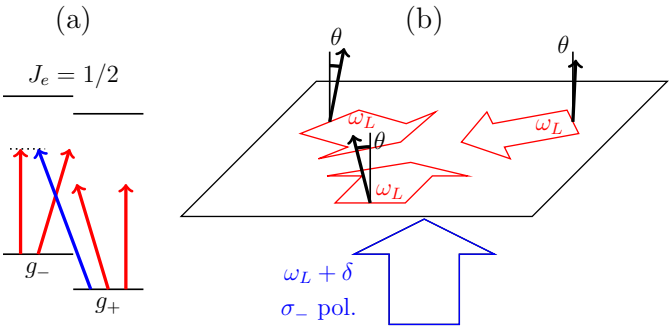

Fig. 1: (Colour on-line) (a) A ground level with angular momentum $J_g = 1/2$ is coupled to an excited level also with angular momentum $J_e = 1/2$ by laser beams at frequency ω_L and $\omega_L + \delta$. The Zeeman splitting between the two ground states $g_\pm$ is δ. (b) Three linearly polarized beams at frequency ω_L with equal intensity and with wave vectors at an angle of $2\pi/3$ propagate in the xy-plane. The beams are linearly polarized at an angle θ to the z-axis. The fourth, circularly polarized beam at frequency $\omega_L + \delta$ propagates along the z-axis.

of the additional laser at $\omega_L + \delta$. This beam is assumed to be a plane wave propagating along z, so that E is a uniform, adjustable coupling. The ac Stark shift due to this additional laser is incorporated in the definition of δ.

We consider the laser configuration represented in fig. 1(b). The laser field at frequency ω_L is formed by the superposition of three plane travelling waves of equal intensity with wave vectors $\boldsymbol{k}_i$ in the xy-plane. We focus on a situation of triangular symmetry, in which the three beams make an angle of $2\pi/3$ with each other, $\boldsymbol{k}_1 = -k/2\,(\sqrt{3}, 1, 0)$, $\boldsymbol{k}_2 = k/2\,(\sqrt{3}, -1, 0)$ and $\boldsymbol{k}_3 = k(0, 1, 0)$. Each beam is linearly polarized at an angle θ to the z-axis, which leads to

$$\boldsymbol{\kappa} = \kappa \sum_{i=1}^{3} e^{i\boldsymbol{k}_i\cdot\boldsymbol{r}}[\cos\theta\,\hat{\boldsymbol{z}} + \sin\theta\,(\hat{\boldsymbol{z}} \times \hat{\boldsymbol{k}}_i)], \tag{3}$$

where κ is the Rabi frequency of a single beam. In the following we denote $\mathcal{V} = \hbar\kappa^2/(3\Delta)$ the energy associated with the atom-light interaction and $\epsilon = E/\kappa$ the relative amplitude of the $\omega_L + \delta$ field with respect to the ω_L field. The recoil energy $E_{\rm R} = \hbar^2k^2/2M$ sets the characteristic energy scale of the problem.

The coupling $\hat{V}$ is written in eq. (2) as the sum of the scalar part $\hbar\kappa_{\rm tot}^2/(3\Delta)\,\hat{1}$ and a zero-trace component that can be cast in the form $\hat{W} = \hat{\boldsymbol{\sigma}}\cdot\boldsymbol{B}/2$, where the $\hat{\sigma}_i$ are the Pauli matrices ($i = x, y, z$). For $E \neq 0$ and $\sin 2\theta \neq 0$, the coupling $\boldsymbol{B}$ is everywhere non-zero. Suppose that the atom is prepared in the local eigenstate $|\chi(\boldsymbol{r})\rangle$ of $\hat{W}$, with a maximal angular momentum projection along $\boldsymbol{n} = -\boldsymbol{B}/|\boldsymbol{B}|$. Suppose also that it moves sufficiently slowly to follow adiabatically this eigenstate, which is valid when $\mathcal{V} \gg E_{\rm R}$. This leads to the Berry's-phase–related gauge potential $i\hbar\langle\chi|\boldsymbol{\nabla}\chi\rangle$, representing a non-zero effective magnetic flux density [14]. For most optical lattice configurations, the periodic variation of

the atom-laser coupling leads to a zero net flux of the effective field through a unit cell of the lattice. Indeed the periodicity of the eigenstate $|\chi\rangle$ entails that the line integral of $\langle\chi|\boldsymbol{\nabla}\chi\rangle$ on the edges of the unit cell vanishes. However this reasoning may fail if the vector potential has singularities inside the cell: this is the so-called *flux lattice* scheme [7].

The singularities of $\langle\chi|\boldsymbol{\nabla}\chi\rangle$ occur at places where the g_+–g_- coupling ($\propto\kappa_0$, see eq. (2)) vanishes. Here, the zeroes of κ_0 are located on a honeycomb lattice, with a distance of $2\lambda/(3\sqrt{3})$ between nearest neighbours, where $\lambda=2\pi/k$ [15]. The unit cell of this hexagonal lattice has an area $A_{\rm cell}=2\lambda^2/(3\sqrt{3})$, and contains two inequivalent sites that correspond to vortices and antivortices of (n_x,n_y), respectively. We will introduce later a gauge transformation that allows one to use the same unit cell for the periodic coupling $\hat{V}$. At the location of the (anti)vortices of (n_x,n_y), the modulus of $B_z\propto|\kappa_+|^2-|\kappa_-|^2$ is maximal and its sign alternates, leading to $n_z=\pm1$. Because the sign of n_z differs for vortices and antivortices, each of these regions wraps the Bloch sphere in the same sense providing the desired rectification of the magnetic flux. The net result is that $\boldsymbol{n}$ wraps the Bloch sphere once within the unit cell, corresponding to $N_\phi=1$ flux quantum. This net flux $N_\phi=1$ is a robust feature of the optical coupling, not relying on fine-tuning of parameters or on the control of the relative phase of the laser beams. Reversal of the magnetic flux ($N_\phi=-1$) can be achieved by changing the sign of the detuning Δ, or replacing the σ_- laser at frequency $\omega_L+\delta$ by a σ_+ laser at frequency $\omega_L-\delta$.

Our laser configuration is reminiscent of the scheme studied in [16]. However in that work only the three beams at frequency ω_L and propagating in the xy-plane were considered. The off-diagonal coupling in $\hat{V}$ is in this case $V_{+-}\propto\kappa_+\kappa_0^*+\kappa_0\kappa_-^*$, and one can check the desired rectification of the magnetic flux at the zeroes of V_{+-} does not occur. Therefore, although the Berry's-phase–related magnetic field found in [16] is locally non-zero, the flux per unit cell vanishes.

In the adiabatic limit, valid for $\mathcal{V}\gg E_{\rm R}$ [6], the atoms are strongly confined to the sites where $\hbar\kappa_{\rm tot}^2/(3\Delta)-|\boldsymbol{B}|/2$ is minimum. Depending on the sign of Δ and the values of θ and E, these sites coincide either with the vertices of the hexagons of the honeycomb lattice introduced above, or with the centre of these hexagons, forming thus a triangular lattice. Both of these tight-binding limits are situations in which the number of flux quanta per hexagonal (respectively, triangular) plaquette is integer (respectively, half-integer), *i.e.* time-reversal symmetry is preserved[1].

In particular in this adiabatic limit the various energy bands cannot have a non-zero Chern number [8]. However, an important aspect of the physics of optical flux lattices is that they do not rely on the adiabatic limit, and can be applied in regimes of intermediate coupling $\mathcal{V}\sim E_{\rm R}$. Indeed the optical flux lattices described here, and those of [7], lead to bands with non-zero Chern number in the weak-coupling limit $\mathcal{V}\lesssim E_{\rm R}$. In this regime, a tight-binding model is inappropriate; departures from this (with next-nearest-neighbour tunnelling and beyond) allow the atoms to perform loops that enclose flux that breaks time-reversal symmetry. That the optical flux lattice scheme applies beyond the tight-binding limit clearly distinguishes this approach from previous proposals for lattice-based gauge fields, which imprint Peierls phases on the tunneling matrix elements for atoms moving in deep optical lattices. (For a review see [6].)

We have calculated the band structures for arbitrary $\mathcal{V}/E_{\rm R}$ by numerical diagonalization of the Hamiltonian (1). To do so, it is helpful to expose the full translational symmetry of the system. The matrix $\hat{V}$ is invariant under translations by the vectors $\lambda/\sqrt{3}\,(\pm1,\sqrt{3},0)$, corresponding to a "naive" unit cell of area $2\lambda^2/\sqrt{3}$. One can reduce the size of the unit cell by taking advantage of a unitary transformation by $\hat{U}\equiv\exp(-i\boldsymbol{k}_3\cdot\boldsymbol{r}\,\hat{\sigma}_z/2)$. This state-dependent gauge transformation gives a transformed Hamiltonian

$$\hat{H}'=\hat{U}^\dagger\hat{H}\hat{U}=\frac{(\hat{\boldsymbol{p}}-\hat{\sigma}_z\hbar\boldsymbol{k}_3/2)^2}{2M}+\hat{V}', \tag{4}$$

where $\hat{V}'=\hat{U}^\dagger\hat{V}\hat{U}$ is of the same form as $\hat{V}$, but with κ_0 replaced by $\kappa_0'=e^{-i\boldsymbol{k}_3\cdot\boldsymbol{r}}\kappa_0$. The advantage is that the coupling $\hat{V}'$ involves only the momentum transfers $\boldsymbol{K}_{1,2}\equiv\boldsymbol{k}_{1,2}-\boldsymbol{k}_3$. Using the momentum transfers to define the reciprocal lattice vectors leads to the largest possible Brillouin zone, and smallest real space unit cell, which coincides with the unit cell of the scalar potential described above, with area $A_{\rm cell}=2\lambda^2/(3\sqrt{3})$. From the Bloch states obtained by exact diagonalization we determine the Chern number of each band using standard techniques [17].

For the special case $\epsilon=\theta=0$, the atoms only experience the scalar potential $\propto|\kappa_0|^2$. For $\Delta>0$, this situation was investigated in detail in [15], in connection with graphene physics (see also [18]). As explained above, $|\kappa_0|^2$ has minima at the sites of a honeycomb lattice. For $\mathcal{V}\gtrsim E_{\rm R}$ one therefore expects the atoms in both $g_\pm$ states to have the low-energy bands of the honeycomb lattice with two Dirac points in the Brillouin zone. One difference with respect to graphene is that, due to the state-dependent gauge transformation $\hat{U}$, the momenta of the two spin states are offset by $\pm\boldsymbol{k}_3/2$. This has the effect that there are three special points in the Brillouin zone: a Dirac point for g_+, a Dirac point for g_-, and a (coincident) Dirac point for both $g_\pm$. The bands are shown in fig. 2 with dotted lines for a cut through the Brillouin zone that passes through these three points.

Perturbations to this decoupled limit cause the Dirac points to split, with consequences that depend on the symmetries that are broken and the relative sizes of the perturbations [19]. For small non-zero θ, the terms $|\kappa_+|^2-|\kappa_-|^2\propto\theta^2$ in (2) break the sublattice symmetry of the honeycomb lattice for both $g_\pm$. Gaps then open in the

[1] In both cases, the unit cell of the lattice contains $N_\phi=1$ flux quantum.

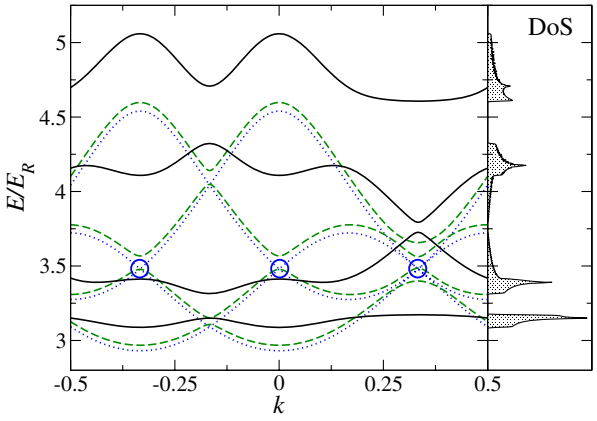

Fig. 2: (Colour on-line) Left-hand panel: band structure for $F = 1/2$ for $\mathcal{V} = 1.8\,E_{\rm R}$ along a path $\boldsymbol{k} = k(\boldsymbol{K}_2 - 2\boldsymbol{K}_1) - \boldsymbol{k}_3/2$ through the Brillouin zone. For $\epsilon = \theta = 0$ (dotted blue line), the decoupled $m = \pm 1/2$ states each have two Dirac points, indicated by circles. For weak coupling $\epsilon = \theta = 0.1$ (dashed green line) the Dirac points split in a manner that breaks time-reversal symmetry, giving the lower two bands a net Chern number of 1. For intermediate coupling $\epsilon = 0.4$, $\theta = 0.3$ (solid black line) the lowest energy band has Chern number 1. Right-hand panel: the density of states for $\mathcal{V} = 1.8\,E_{\rm R}$, $\epsilon = 0.4$ and $\theta = 0.3$.

spectrum at the locations of the Dirac points. For $\epsilon = 0$ the lower two bands separate from the upper two bands in such a way that both pairs of bands are topologically trivial, that is each pair has net Chern number of zero. When both ϵ and θ are non-zero, the optical dressing leads to a net flux through the unit cell, indicating time-reversal symmetry breaking. Indeed, we find that for $\epsilon, \theta \neq 0$ the bands can acquire non-zero Chern numbers. Specifically, in the perturbative limit ($\epsilon, \theta \ll 1$) the Dirac points split in such a way that the lower two bands have a net Chern number of 1 provided θ^2/ϵ is sufficiently small. When θ^2/ϵ exceeds a certain value ($\simeq 0.19$ for $\mathcal{V} = 1.8\,E_{\rm R}$) there is a transition to the topologically trivial case described above. Beyond the perturbative limit, as the couplings ϵ and θ increase, the splitting between the lower two bands increases and the lowest energy band evolves into a narrow band with Chern number 1. An example is shown by the solid lines and density of states in fig. 2, for which the lowest band has a width $\Delta E \simeq 0.1 E_{\rm R}$. The optical dressing (2) affords a great deal of freedom to tune parameters to reduce the ratio of the bandwidth of the lowest band to the gap to the next band. For example, for $\mathcal{V} = 2E_{\rm R}$, $\theta = \pi/4$, $\epsilon = 1.3$, the lowest band has a width of only $\Delta E \simeq 0.01 E_{\rm R}$ and is separated from the next band by about $0.4\,E_{\rm R}$ (see fig. 3).

It is important to emphasize that the formation of this narrow low-energy band is not simply due to compression into a tight-binding band[2]. Rather it is closely related

[2] For a tight-binding band in the limit of vanishing tunnel coupling when the Wannier states become exponentially localized, the Chern number of the band must be zero [20], or a set of bands with net Chern number zero must become degenerate.

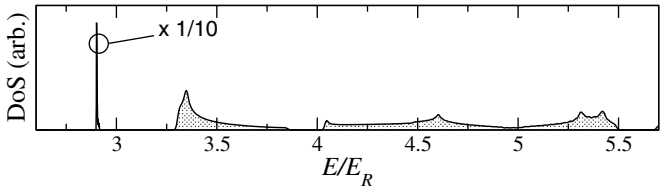

Fig. 3: Density of states for $F = 1/2$ for $\mathcal{V} = 2E_{\rm R}$, $\theta = \pi/4$, $\epsilon = 1.3$. The lowest band has Chern number 1, a width of about $0.01 E_{\rm R}$, and is well separated in energy from the next band. The density of states for the lowest band has been rescaled by $1/10$.

to the formation of Landau levels in a uniform magnetic field. A continuum Landau level is highly degenerate, with degeneracy equal to the number of flux quanta piercing the plane. Thus, for the flux density here, of one flux quantum per unit cell, a Landau level would have one state per unit cell: that is one band within the Brillouin zone. The lowest band of figs. 2 and 3, with its narrow width and Chern number of 1, is the optical flux lattice equivalent of the lowest Landau level.

The above scheme can be generalized to atoms of the alkali-metal family, whose ground state $nS_{1/2}$ is split into two hyperfine levels $I \pm 1/2$, where I is the nuclear spin. The laser excitation is tuned in this case around the resonance lines D_1 (coupling to $nP_{1/2}$ with detuning Δ_1) and D_2 (coupling to $nP_{3/2}$ with detuning Δ_2). Let us focus here on the lowest hyperfine level $F = I - 1/2$. For the configuration of fig. 1 the atom-laser coupling can be written

$$\hat{V} = \frac{\hbar \kappa_{\rm tot}^2}{\bar{\Delta}} \hat{1} + \hat{\boldsymbol{F}} \cdot \boldsymbol{B}, \tag{5}$$

where $\bar{\Delta}^{-1} = (1/3)\Delta_1^{-1} + (2/3)\Delta_2^{-1}$, $\hat{\boldsymbol{F}}$ is the angular momentum operator in the ground state manifold in units of $\hbar$, and

$$B_x + iB_y = \xi\, E \kappa_0, \qquad B_z = \xi\,(|\kappa_-|^2 - |\kappa_+|^2), \tag{6}$$

with $\xi = (\Delta_2^{-1} - \Delta_1^{-1})\hbar/[3(F+1)]$. Under the unitary transformation $\hat{U} \equiv \exp(-i\boldsymbol{k}_3 \cdot \boldsymbol{r} \hat{F}_z)$ the Hamiltonian takes a similar form to (4), now with $\hat{\sigma}_z/2$ replaced by $\hat{F}_z$, and again with a coupling $\hat{V}'$ in which κ_0 is replaced by $\kappa_0' = e^{-i\boldsymbol{k}_3 \cdot \boldsymbol{r}} \kappa_0$ giving the unit cell of the honeycomb lattice as before. Adiabatic motion of the atom still leads to a dressed state with angular momentum along the vector $\boldsymbol{n}$ that wraps the Bloch sphere once in the unit cell. However, now the Berry phase acquired is larger by a factor of $2F$ [14]. Therefore, the unit cell contains $N_\phi = 2F$ flux quanta. This increase of N_ϕ leads to an important new feature: a continuum Landau level now corresponds to $N_\phi = 2F$ states per unit cell. Thus, the analogue of the lowest Landau level is a set of $2F$ low-energy bands with a net Chern number of 1. Spatial variations in the scalar potential and flux density will cause these bands to split and to acquire non-zero widths.

We shall illustrate the physics for $F > 1/2$ by describing the properties for bosonic atoms with $F = 1$. This is a very

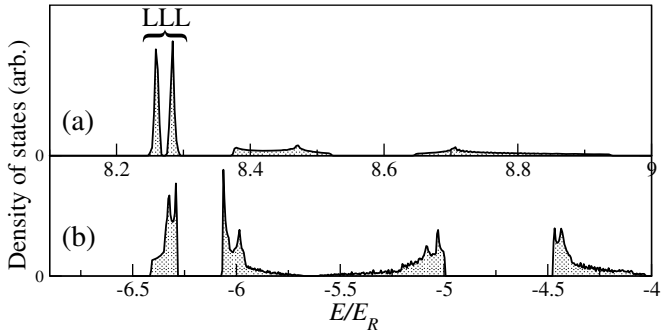

Fig. 4: Density of states for $F=1$. (a) $\mathcal{V}=8\,E_{\rm R}$, $\epsilon=0.8$, $\theta=0.2$, $\gamma_1=0$, $\gamma_2=-0.15\,E_{\rm R}$. The two lowest bands have Chern numbers of -1 and 2. Taken together, these are analogous to the lowest Landau level (LLL). (b) $\mathcal{V}=2\,E_{\rm R}$, $\epsilon=3$, $\theta=0.5$, $\gamma_1=10E_{\rm R}$, $\gamma_2=-10E_{\rm R}$. The system behaves as a two-level system formed from $m=0,-1$. The lowest-energy band is analogous to the LLL.

important case, as it applies for example to the hyperfine ground states of ^{23}Na, ^{39}K, and ^{87}Rb. In order to control the respective role of the various Zeeman sublevels, we also include in the Hamiltonian the additional Zeeman coupling to an external magnetic field

$$\hat{W}_\gamma=\gamma_1\hat{F}_z+\gamma_2(1-\hat{F}_z^2), \tag{7}$$

where γ_1 and γ_2 correspond to the linear and quadratic Zeeman effects, respectively. For simplicity we assume that $|\Delta_1|\ll|\Delta_2|$ and we take into account only the coupling between the ground state and the $P_{1/2}$ excited state (D_1 line). As above, we characterize the atom-laser coupling by the angle θ and the two dimensionless parameters $\epsilon=E/\kappa$ and $\mathcal{V}/E_{\rm R}$, where $\mathcal{V}=\hbar\kappa^2/(3\Delta_1)$.

For a state-independent potential ($\epsilon=\theta=\gamma_1=\gamma_2=0$) and positive detuning Δ_1, each of the three states $|F=1,m\rangle$ with $m=0,\pm1$ experiences a honeycomb lattice potential and has two Dirac points. Now the offsets in wave vector are such that there are three special $\boldsymbol{k}$-points, at each of which two Dirac points coincide. Again the Dirac points are split by perturbations that break time-reversal symmetry ($\epsilon,\theta\neq0$) and the lowest three bands can acquire non-zero Chern number. Differences from $F=1/2$ emerge in the regime of intermediate coupling. In particular we find a domain in parameter space where the two lowest-energy bands are closely spaced, with narrow total width and a net Chern number of 1 (see fig. 4(a)). This confirms the expectation mentioned above that the set of the $2F=2$ lowest bands constitutes in this case the analogue to the lowest Landau level. One can also make use of the quadratic Zeeman splitting $\gamma_2\neq0$ to arrange situations in which only two of the m-states contribute. This two-level system is then of the same form as $F=1/2$. In this case, parameters can be chosen to form a single narrow lowest-energy band with Chern number 1, which by itself is analogous to the lowest Landau level. An example is presented in fig. 4(b), showing similar features to $F=1/2$ (fig. 2).

These narrow bands with non-zero Chern number are excellent systems with which to explore strong-correlation phenomena related to fractional quantum Hall physics [3], both for fermions and bosons. Given the contact nature of interactions in ultracold atomic gases, one might think that the Pauli principle would prevent interparticle interactions between fermions within a single band. Interactions would indeed vanish if the atoms were to move adiabatically, since then, at each point in space, only a single dressed state would be relevant. However, non-adiabatic effects lead to residual interactions between fermions. In a semi-classical picture, one can imagine two atoms that approach the same point in space from different directions. Since the motion is non-adiabatic, when they reach that point they can be in different internal states, so there is some probability that they coincide and interact.

To understand quantitatively how non-adiabatic motion of the fermions leads to interparticle interactions within a single band, consider a system of spin-1/2 fermions ($m=\pm1/2$) with spin-independent contact potential $V_{m,m'}(\boldsymbol{r},\boldsymbol{r}')=g_{\rm 2D}\delta^2(\boldsymbol{r}-\boldsymbol{r}')$. The mean interaction energy for any Fock state is

$$\begin{aligned}\langle\hat{H}_I\rangle &= \frac{1}{2}g_{\rm 2D}\int\sum_{m,m'}\left[\rho_{m,m}\rho_{m',m'}-|\rho_{m,m'}|^2\right]\mathrm{d}^2r\\ &= \frac{1}{4}g_{\rm 2D}\int\rho^2(\boldsymbol{r})\left[1-P^2(\boldsymbol{r})\right]\mathrm{d}^2r,\end{aligned} \tag{8}$$

where $\rho_{m,m'}(\boldsymbol{r})\equiv\langle c_m^\dagger(\boldsymbol{r})c_{m'}(\boldsymbol{r})\rangle$ and $c_m^\dagger(\boldsymbol{r})$ creates a particle at $\boldsymbol{r}$ in spin state m. In eq. (8) we have introduced the local total density ρ and local polarization P (in units of $\hbar/2$). In the adiabatic limit, the local polarization is everywhere maximal, $P=1$, so the interaction energy vanishes. However, for non-adiabatic motion the local polarization is reduced and the interaction energy is non-zero.

We quantify the size of the interactions by considering a filled band. Then $\rho_{m,m'}(\boldsymbol{r})=\sum_{\boldsymbol{k}}\left[\phi_m^{\boldsymbol{k}}(\boldsymbol{r})\right]^*\phi_{m'}^{\boldsymbol{k}}(\boldsymbol{r})$, where $\phi_m^{\boldsymbol{k}}(\boldsymbol{r})$ is the space- and spin-dependent wave function of the Bloch state $\boldsymbol{k}$ in this band. We define an interaction parameter $I\equiv\langle H_I\rangle/E_0$ with $E_0\equiv(1/4)g_{\rm 2D}\int\rho^2\,\mathrm{d}^2r$ the mean energy for $P=0$. We have computed the total interaction energy for the lowest-energy band in fig. 2 for each of the three cases[3] of (ϵ,θ). For $\epsilon=\theta=0$ the two spin states are decoupled, so the lowest band is unpolarized ($P=0$) and $I=1$. For weak coupling $\epsilon=\theta=0.1$ we find $I=0.95$, showing a (small) suppression of interactions. With increasing coupling, the interactions continue to be suppressed. However, even for intermediate coupling ($\epsilon=0.4$, $\theta=0.3$), where the lowest band has become narrow, the interaction parameter is $I=0.42$, showing that the motion is still far from adiabatic. The ultra-narrow band shown in fig. 3 has a small value for the interaction parameter $I=0.046$.

[3]Although in the first two cases there is an energy overlap with the second band, one can still compute the interaction energy for the Fock state in which the lowest-energy band is filled.

Since the low-energy bands described above are analogous to the lowest Landau level, leading candidates for strongly correlated phases include the Laughlin states, at mean particle densities of $\bar{\rho} = (1/3)N_\phi/A_{\rm cell}$ for fermions and $\bar{\rho} = (1/2)N_\phi/A_{\rm cell}$ for bosons, with $N_\phi = 2F$; or, if the quadratic Zeeman effect is used to isolate an effective two-level system, with $N_\phi = 1$. Strongly correlated phases of this kind are energetically competitive when the mean interaction energy is on the scale of the bandwidth, which we denote $\Delta E \equiv \alpha_1 E_{\rm R}$, introducing a numerical factor α_1 that is small for the narrow bands described above. For bosons, we take the typical scale for interactions to be the interaction contribution to the chemical potential for a condensate formed from the lowest energy single particle state, $E_{\rm i} = g_{\rm 2D}\int \rho^2 \, {\rm d}^2 r / \int \rho \, {\rm d}^2 r \equiv \alpha_2 g_{\rm 2D}\bar{\rho}$, with α_2 a numerical factor that accounts for wave function localization close to the lattice sites. For the Laughlin state, this gives $E_{\rm i}/\Delta E = (3\sqrt{3}N_\phi/8\pi^2)(\alpha_2/\alpha_1)\tilde{g}$, where $\tilde{g} = M g_{\rm 2D}/\hbar^2$ is the dimensionless interaction strength in 2D. Taking the parameters of fig. 4(a) ($N_\phi = 2$, $\alpha_1 \simeq 0.05$, $\alpha_2 \simeq 3.3$) this is $E_{\rm i}/\Delta E \simeq 9\tilde{g}$. With cold atomic gases confined in a strong one-dimensional optical lattice along the z-direction, values of $\tilde{g}$ can approach unity [21], so that reaching the strongly correlated regime can be realistically envisaged. For spin-1/2 fermions, the partial suppression of s-wave interactions discussed above somewhat complicates the realization of the correlated regime. However one can rely on Feshbach resonances to produce a strongly interacting 2D Fermi gas [22], and thus also in this case reach the point where $\langle H_I \rangle \sim \Delta E$. Note that in the case of ^{171}Yb or ^{199}Hg, one has to turn to optically induced Feshbach resonances [23,24], because the spin of the ground state has a purely nuclear origin hence "standard" magnetic Feshbach resonances do not occur.

The appearance of fractional quantum Hall states is predicted to lead to various consequences for the ground state and excitation spectrum of the cold atomic gas, as discussed in the literature [1–3]. Perhaps the most evident feature is a plateau (or plateaus) in *in situ* images of the density of a trapped gas, arising from the incompressibility of the FQH states. For the Laughlin states, these plateaus are expected at mean densities for which there is no competing Mott insulator state.

In summary we have presented a simple scheme by which optical flux lattices can be implemented using two-photon dressed states. The method applies to commonly studied atomic species, requires few lasers, and uses only well-established techniques. Our studies show that for practical parameters, the non-adiabatic character of atomic motion can lead to significant interactions even for fermions occupying a single band. This scheme should allow experiments on cold atomic gases to explore strong correlation phenomena in regimes of flux density previously unattainable.

* * *

This work was supported by EPSRC Grant EP/F032773/1, IFRAF, ANR (BOFL project), and E.U. (MIDAS project). JD acknowledges useful discussions with F. Gerbier and N. Goldman.

REFERENCES

[1] Bloch I., Dalibard J. and Zwerger W., *Rev. Mod. Phys.*, **80** (2008) 885.
[2] Fetter A. L., *Rev. Mod. Phys.*, **81** (2009) 647.
[3] Cooper N. R., *Adv. Phys.*, **57** (2008) 539.
[4] Lin Y.-J., Compton R. L., Jiménez-García K., Porto J. V. and Spielman I. B., *Nature*, **462** (2009) 628.
[5] Lewenstein M., Sanpera A., Ahufinger V., Damski B., De A. S. and Sen U., *Adv. Phys.*, **56** (2007) 243.
[6] Dalibard J., Gerbier F., Juzeliūnas G. and Öhberg P., arXiv:1008.5378 (2010).
[7] Cooper N. R., *Phys. Rev. Lett.*, **106** (2011) 175301.
[8] Thouless D. J., Kohmoto M., Nightingale M. P. and den Nijs M., *Phys. Rev. Lett.*, **49** (1982) 405.
[9] Taie S., Takasu Y., Sugawa S., Yamazaki R., Tsujimoto T., Murakami R. and Takahashi Y., *Phys. Rev. Lett.*, **105** (2010) 190401.
[10] Yi L., Mejri S., McFerran J. J., Le Coq Y. and Bize S., *Phys. Rev. Lett.*, **106** (2011) 073005.
[11] Porsev S. G., Derevianko A. and Fortson E. N., *Phys. Rev. A*, **69** (2004) 021403.
[12] Bigeon M.-C., *J. Phys.* (*Paris*), **28** (1967) 51.
[13] Cohen-Tannoudji C., Dupont-Roc J. and Grynberg G., *Atom-Photon Interactions* (Wiley, New York) 1992.
[14] Berry M. V., *Proc. R. Soc. London, Ser. A*, **392** (1984) 45.
[15] Lee K. L., Grémaud B., Han R., Englert B.-G. and Miniatura C., *Phys. Rev. A*, **80** (2009) 043411.
[16] Dudarev A. M., Diener R. B., Carusotto I. and Niu Q., *Phys. Rev. Lett.*, **92** (2004) 153005.
[17] Fukui T., Hatsugai Y. and Suzuki H., *J. Phys. Soc. Jpn.*, **74** (2005) 1674 (cond-mat/0503172).
[18] Górecka A., Grémaud B. and Miniatura C., arXiv:1105.3535 (2011).
[19] Haldane F. D. M., *Phys. Rev. Lett.*, **61** (1988) 2015.
[20] Thouless D. J., *J. Phys. C*, **17** (1984) L325.
[21] Hadzibabic Z. and Dalibard J., *Riv. Nuovo Cimento*, **34** (2011) 389 (arXiv:0912.1490).
[22] Fröhlich B., Feld M., Vogt E., Koschorreck M., Zwerger W. and Köhl M., *Phys. Rev. Lett.*, **106** (2011) 105301.
[23] Enomoto K., Kasa K., Kitagawa M. and Takahashi Y., *Phys. Rev. Lett.*, **101** (2008) 203201.
[24] Reichenbach I., Julienne P. S. and Deutsch I. H., *Phys. Rev. A*, **80** (2009) 020701.